

Multi-user adaptive orthogonal frequency-division multiplexing system for indoor wireless optical communications

O. González, S. Rodríguez, R. Pérez-Jiménez, F. Delgado and A. Ayala

Abstract: An adaptive orthogonal frequency-division multiplexing (OFDM) system is proposed for multi-user communications over indoor wireless optical channels. The designed system uses multi-user least-squares detection techniques applied to space-division multiple access and OFDM schemes, in conjunction with angle-diversity reception. The system, which does not present an excessive increase in complexity with respect to the previous schemes, can support high bit rates for multiple users, beyond 100 Mbits/s. It also mitigates the channel fluctuations induced when either the space distribution or the number of emitters and receivers varies. The performance of the new proposed scheme is compared with that of a non-adaptive multi-user system and an adaptive single-user system, both described in the previous works, when they face similar environmental situations. The obtained results show a significant enhancement with respect to both the previous multi-user system and the adaptive single-user one, since the new scheme allows adaptively managing the system throughput on a multi-user environment.

1 Introduction

Non-directed infrared (IR) radiation has been considered as a very attractive alternative to radio frequency (RF) waves for indoor wireless local area networks [1]. The pioneer research studies were carried out on diffuse link configurations [2–6]. The diffuse link configuration establishes a non-directed non-line-of-sight link, projecting a wide beam on a reflecting surface, for example ceiling, and having a receiver with a wide field of view (FOV) face towards that surface, which alleviates the problem of aligning transmitters and receiver and makes the system robust against blockage. However, an immediate disadvantage of a diffuse IR channel is its increased path loss due to the lack of a direct link between transmitter and receiver. Several works have proposed the use of power-efficient signalling schemes such as pulse-position modulation (PPM), which allows to increase the transmit power in order to compensate for path loss [7]. Nevertheless, the limited bandwidth of the channel due to multipath dispersion caused by reflections of light from walls and room objects creates intersymbol interference (ISI) when signals at high bit rates are transmitted over the channel. Fluorescent light interference is another major problem on indoor wireless IR communications systems, since it induces severe narrowband interference to baseband modulation schemes commonly used such as on-off keying and PPM. Spread spectrum techniques have been proposed in order to

reduce the multipath-dispersion induced penalty over transmission baud rate and narrowband interference effects, but the processing gain of these schemes reduces the system bandwidth efficiency [8]. The effect of ISI can also be eliminated by using a multibeam transmitter in conjunction with a multiple element, narrow FOV direction-diversity (also known as angle-diversity) receiver [9–11]. The transmitter in this configuration projects the light power in the form of multiple narrow beams of equal intensity over several small areas (spots) on a diffusing surface such as the ceiling. Thus each diffusing spot may be considered a line-of-sight source, which can be aimed at a narrow FOV receiving branch. With this arrangement, only a finite number of spots, that is signal paths, are seen by the receiving branch. As the branch FOV is decreased, a smaller number of spots can be sighted and in the limiting case in which only one spot is seen, channel behaves as nearly ideal.

In the last years, significant interest has focused on modulation techniques, which can provide broadband transmission over wireless IR channels. The main requirements looked for in the modulation technique are the ability to combat ISI and narrowband interference, and the availability of a high bandwidth efficiency. Multi-carrier modulation techniques, including orthogonal frequency-division multiplexing (OFDM), are among the more satisfactory solutions to this problem [12, 13]. Another interesting field under investigation is the multi-access communication. In wireless RF applications, there exist many works that address this issue. Many solutions have been studied for multi-user communications, from the use of conventional schemes such as time-division multiple access or frequency-division multiple access in conjunction with the OFDM technique, or schemes that combine multi-carrier OFDM transmissions with code-division multiple access [14]. Recently, a multiple access technique known as space-division multiple access (SDMA) has also drawn wide interest. This technique exploits the unique, user-specific

© The Institution of Engineering and Technology 2007

doi:10.1049/iet-opt:20060020

Paper first received 16th February and in revised form 24th July 2006

O. González, S. Rodríguez, F. Delgado and A. Ayala are with the Department of Fundamental and Experimental Physics, Electronics and Systems, University of La Laguna, La Laguna, Tenerife, Canary Islands, 38203, Spain

R. Pérez-Jiménez is with the Department of Signals and Communications, University of Las Palmas de Gran Canaria, Las Palmas de Gran Canaria, Canary Islands, 35017, Spain

E-mail: oghdez@ull.es

‘spatial signature’ of the individual users to differentiate among them [15]. The receiver is constituted by several antenna elements and different multi-user detection techniques can be applied to demodulate the information relative to the desirable user [16, 17].

2 Optical channel model

There are several simulation models used to estimate the impulse response of IR wireless indoor channels. We have selected a Monte Carlo based ray-tracing algorithm [6, 18, 19]. In the algorithm, every ray is generated at emitter position with a probability distribution equal to its radiation pattern. The power of each generated ray is initially the source power (normalised to 1 W) divided by the number of rays used to discretise the source. When a ray impinges on a surface, the reflection point is converted into a new optical source, thus a new ray is generated with a probability distribution provided by the reflection pattern of that surface. The process continues during the simulation time. After each reflection, the power of the ray is reduced by the reflection coefficient (ρ) of the surface, and the reflected power which reaches the j th branch of receiver ($p_{j,i,k}$, i th ray, k th time interval) is computed. The Phong’s model was used to describe the reflection pattern of surfaces [5]. This model is able to approximate the behaviour of those surfaces that present a strong specular component: it takes into account the reflection pattern as the sum of both diffuse and specular components. Therefore surface characteristics are defined by two new parameters: the percentage of incident signal that is reflected diffusely r_d and the directivity of the specular component of the reflection m . The total received power at the j th branch of the IR detector ($j = 1, \dots, P$) in the k th time interval (width Δt) is computed as the sum of the power of the $N_{j,k}$ rays that contribute in that interval

$$p_{j,k} = \sum_{i=1}^{N_{j,k}} p_{j,i,k} \quad (1)$$

Since we have adopted a receiver responsivity of 1 A/W, the impulse response $h_j(t)$ at all branches ($j = 1, \dots, P$) is given by

$$h_j(t) = \sum_{k=0}^{K-1} p_{j,k} \delta(t - k\Delta t) \quad (2)$$

where $K = t_{\max}/\Delta t$, and we have assumed as the time origin the instant when the rays are generated from emitters. The previous process can be repeated to obtain the impulse response at all branches for different positions of the emitter, when multi-user transmission is considered.

3 Optical adaptive SDMA–OFDM system model

The block diagram of the indoor wireless optical adaptive SDMA–OFDM system for multi-user communications is shown in Fig. 1. The transmitters’ structure of the L users is the same as that proposed for single-user communications in the previous work [13]. First, at the l th user transmitter, $\Sigma_p b_p^{(l)}$ data bits are generated and modulated by S_l $2^{b_p^{(l)}}$ -QAM (quadrature amplitude modulation) modulators (S_l subcarriers, $b_p^{(l)}$ is the number of bits conveyed by the p th subcarrier). Then, $N - S_l$ zeros (one of them before, corresponding to the direct current (DC) value) are padded to the S_l symbols generated by the modulators, and the complex conjugate of the mirror of the word of N

symbols is added to the latter before computing the inverse fast Fourier transform (IFFT). The outgoing IFFT symbol is a real sequence of $2N$ points and it can drive directly the light sources after adding an appropriate DC offset to avoid lower clipping. Moreover, a cyclic prefix is inserted (a quasi-periodic extension of $S - 2N$ samples) to combat ISI. The symbol duration is $T_s = (1/\Delta f)$ seconds (with the subcarriers Δf hertz far apart), and in this time S samples are transmitted. Each transmitted signal is distorted by channel response (channel plus transmitter lowpass and receiver antialiasing filters) and corrupted by noise (channel noise, preamplifier thermal noise, photodiode shot noise at receiver and the noise induced by the sun and illumination lights). The overall noise process is modelled as zero-mean additive white Gaussian noise (AWGN) with two-sided power spectral density $N_0/2$.

The multi-user receiver presents a bank of P identical receiving branches. Each receiving branch is provided with an OFDM demodulator, at the output of its photodetector. In each of them, once the corrupted cyclic prefix is removed, the fast Fourier transform (FFT) of $2N$ points is computed. Only the first S_l points (after DC value), associated to the S_l subcarriers that convey data symbols, are considered. We assume that all transmitters are synchronised, so they initiate the transmission of each OFDM frame at the same time. Therefore the signals of every user reach the receiver almost simultaneously except for the path delay due to the different distances that there exist between users and receiver. The L users’ transmitters and narrow FOV direction-diversity receiver creates a multiple input multiple output channel scenario. Consequently, we have multiple copies of a single subcarrier data symbol received from P separate channels. The multi-user linear detector must separate the transmitted signals associated to the L users with the aid of their unique user-specific spatial signature, constituted by the channel transfer factors between the users’ emitters and the P different receiving branches of the receiver. Fig. 2 shows the structure of the multi-user adaptive detector.

The vector of complex signals, $\mathbf{x}_{p,n}$, received by the P -branch detector array in the p th subcarrier of the n th OFDM symbol is constituted by the superposition of the independently distorted signals associated with the L users sharing the same space-frequency resource. The signal is corrupted by Gaussian noise at the detector array elements. Throughout this paper due to the slow time-varying nature of indoor wireless optical channel, channel response $\mathbf{H}_p(n)$ does not practically change with n and this index will be omitted for notational convenience, yielding

$$\mathbf{x}_p = \mathbf{H}_p \mathbf{s}_p + \mathbf{n}_p \quad (3)$$

where the vector $\mathbf{x}_p \in \mathbb{C}^{P \times 1}$ of received signals at the p th subcarrier ($p = 1, \dots, S_l$), the vector $\mathbf{s}_p \in \mathbb{C}^{L \times 1}$ of transmitted signals and the array noise vector $\mathbf{n}_p \in \mathbb{C}^{P \times 1}$, respectively, are given by

$$\begin{aligned} \mathbf{x}_p &= (x_{1p}, x_{2p}, \dots, x_{pp})^T \\ \mathbf{s}_p &= (s_p^{(1)}, s_p^{(2)}, \dots, s_p^{(L)})^T \\ \mathbf{n}_p &= (n_{1p}, n_{2p}, \dots, n_{pp})^T \end{aligned} \quad (4)$$

The frequency domain channel transfer factor matrix $\mathbf{H}_p \in \mathbb{C}^{P \times L}$ is constituted by the set of channel transfer factor vectors $\mathbf{H}_p^{(l)} \in \mathbb{C}^{P \times 1}$, $l = 1, \dots, L$ of the L users

$$\mathbf{H}_p = (\mathbf{H}_p^{(1)}, \mathbf{H}_p^{(2)}, \dots, \mathbf{H}_p^{(L)}) \quad (5)$$

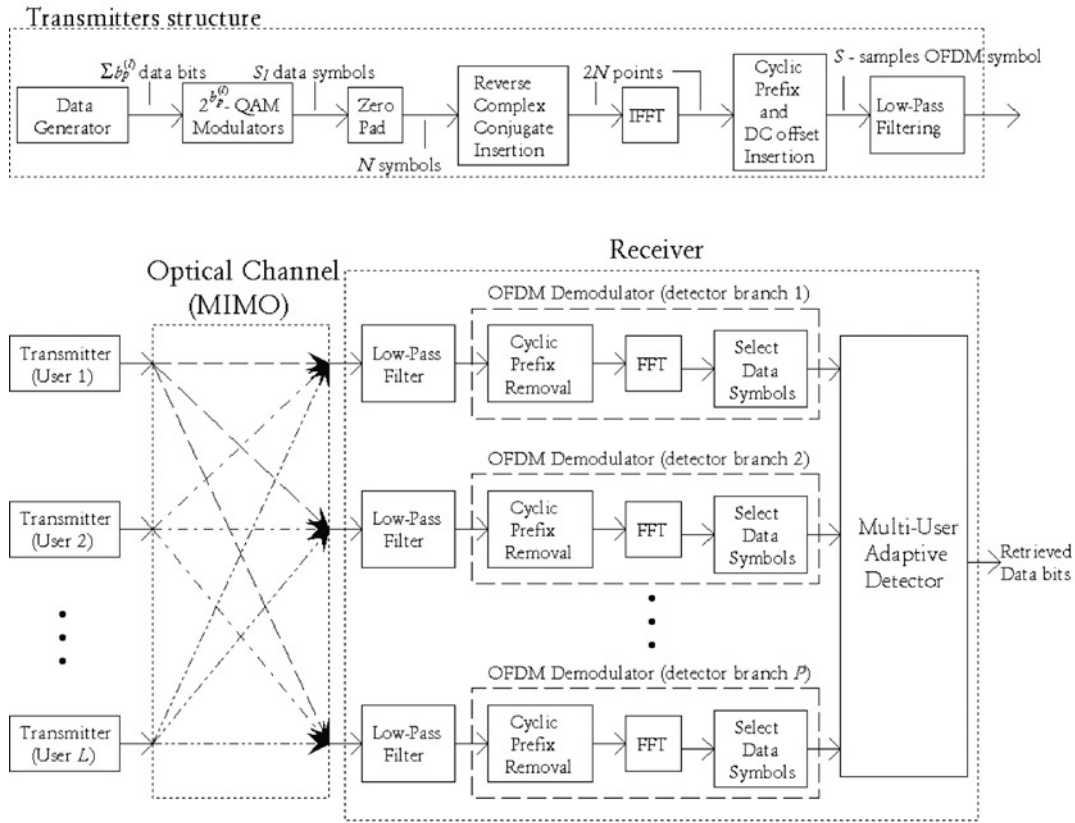


Fig. 1 Adaptive SDMA-OFDM system for multi-user communications over indoor wireless optical channels

each of which hosts the frequency domain channel transfer factors between the single emitter source associated to a particular user l and the receiving branches $j = 1, \dots, P$ at the p th subcarrier band

$$\mathbf{H}_p^{(l)} = (H_{1p}^{(l)}, H_{2p}^{(l)}, \dots, H_{Pp}^{(l)})^T \quad (6)$$

with $l = 1, \dots, L$. At the linear detector, an estimate $\hat{s}_p \in \mathbb{C}^{L \times 1}$ at the p th subcarrier band of the vector of transmitted signals s_p of the L simultaneous users is generated by linearly combining the signals received by the P different receiving branches with the aid of a weight matrix $\mathbf{W}_p \in \mathbb{C}^{P \times L}$

$$\hat{s}_p = \mathbf{W}_p^H \mathbf{x}_p \quad (7)$$

where \mathbf{W}_p^H denotes the complex conjugate matrix of the matrix \mathbf{W}_p . When least-squares (LS) error detector is

considered, the weight matrix $\mathbf{W}_{p,LS} \in \mathbb{C}^{P \times L}$ is given by [15]

$$\mathbf{W}_{p,LS} = \mathbf{H}_p (\mathbf{H}_p^H \mathbf{H}_p)^{-1} \quad (8)$$

It can be observed that the LS detector requires the knowledge of the transfer factor matrix \mathbf{H}_p . The method described in the work of González *et al.* [13, 20] where TS known training sequences are used to estimate the channel transfer function between a single user and the receiver, can be used to estimate the matrix \mathbf{H}_p , assuming that only one user is transmitting during the training periods. If a certain known training sequence X_p ($p = 1, \dots, S_l$) is transmitted by the l th user ($l = 1, \dots, L$) over the slow time-varying wireless optical channel, the channel response of each sub-band $H_{p,j}^{(l)}$ for this user at the j th receiving branch ($j = 1, \dots, P$) can

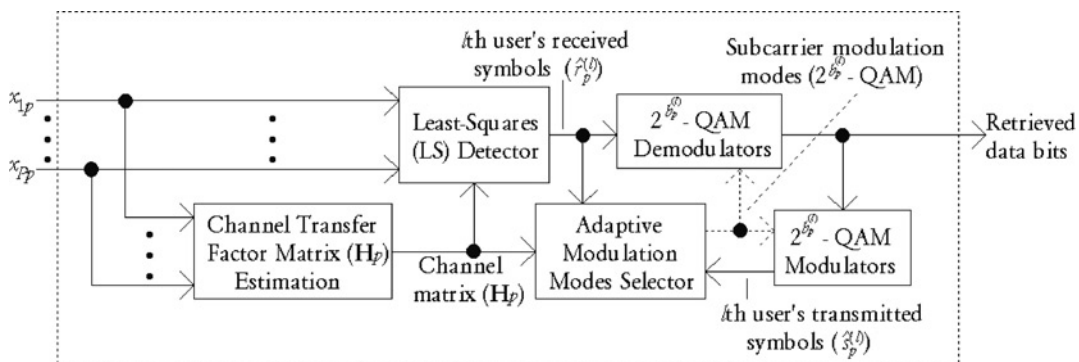


Fig. 2 Multi-user adaptive detector

be estimated from the S_I received symbols ($Y_{j,p}^{(l)}$) as follows

$$\hat{H}_{j,p}^{(l)} = Y_{j,p}^{(l)} / X_p \quad (9)$$

Note that the $\hat{H}_{j,p}^{(l)}$ values are distorted by noise and therefore several training sequences can be transmitted and then the mean values of the estimates can be used to obtain a better channel characterisation.

We have selected the LS detector because other linear detectors, such as the minimum mean-square error (MMSE) detector, require statistical information concerning the transmitted signal variances and the AWGN variance into the detection process. We have probed that both MMSE and LS detectors have almost the same performances over indoor wireless optical channels [21] in spite of the lower implementation complexity of the latter one. Moreover, the MMSE detector can even perform worse when an inadequate estimate of the noise variance is used [21]. On the other hand, the optimum nonlinear maximum likelihood detector does not present an extremely significant performance improvement with respect to linear detectors (signal-to-noise ratio (SNR) gains not greater than 2 dB were observed when quadrature phase-shift keying (QPSK) was used as modulation mode in all subcarriers and $L = 3$ simultaneous users were considered) and it is impractical when 16-QAM or higher modulation modes are applied over the subcarriers [21].

The l th user's associated vector component of estimate (7) of the vector of transmitted signals at the p th subcarrier can be expressed as

$$\hat{s}_{p,LS}^{(l)} = \mathbf{W}_{p,LS}^{(l)H} \mathbf{x}_p \quad (10)$$

where the l th user's associated weight vector $\mathbf{W}_{p,LS}^{(l)} \in \mathbb{C}^{P \times 1}$ coincides with the l th column vector of the matrix $\mathbf{W}_{p,LS}$. The complex symbol that is most likely to have been transmitted by the l th user can be determined upon minimising the Euclidean distance between estimate (10) of the transmitted signal obtained at the l th user's combiner output and all constellation points associated to the specific modulation scheme employed.

Owing to the slow time-varying nature of wireless optical channels, periodically sending several training sequences to estimate the channel response does not represent a meaningful amount of transmission overhead. This task is only run between periods of time in which the transmission of a huge amount of OFDM symbols has been completed. On the other hand, a good knowledge of the channel response can help to make a better use of the channel capacity by means of a subcarrier-by-subcarrier adaptive modulation system. In a wireless optical channel, different subcarriers will undergo different gains for each user. Therefore the modulation mode of each transmission subcarrier, that is the number of bits to transmit by a certain user at each subcarrier, can be adaptively tailored to the channel characteristics. The receiver system has to estimate the instantaneous channel response and then it has to determine the most suitable modulation mode for each transmission subcarrier. It is clear that there is an additional amount of transmission overhead since the receiver system has to notify the transmitters about the number of bits assigned to each subcarrier. However, this does not really represent a problem in an indoor low mobility environment as we have indicated before.

Effective demodulation SNR can be computed at receiver as follows (Fig. 2). After each OFDM symbol demodulation, the retrieved data bits are modulated again and the average SNR of received QAM symbols is computed,

using outgoing QAM modulators symbols as reference (therefore we are assuming error-free transmission). The calculation of the l th user's effective demodulation SNR is given by

$$\overline{\text{SNR}}_{\text{eff}}^{(l)}(\text{dB}) = 10 \log_{10} \frac{\overline{|s_p^{(l)}|^2}}{\overline{|r_p^{(l)} - s_p^{(l)}|^2}} \quad (11)$$

where $s_p^{(l)}$ and $r_p^{(l)}$ are the l th user's transmitted and received (before demodulation) data symbols, respectively. From (11), it can be deduced that the effective SNR is an average over all constituent data symbols ($p = 1, \dots, S_I$) of each received OFDM frame.

The bit error rate (BER) curves of each constituent 2^M-QAM mode can be used to find the SNR values that satisfies a specific target BER requirement [13, 20]. So using a simple extrapolation of the BER curves against SNR obtained over AWGN channel, we can determine the required SNR values for several BER thresholds. These values can be used as switching levels for a subcarrier-by-subcarrier adaptive OFDM system [13, 20]. From (3)–(8), when a LS detector is used, we obtain

$$\hat{\mathbf{s}}_{p,LS} = \mathbf{W}_{p,LS}^H \mathbf{x}_p = \mathbf{s}_p + \mathbf{W}_{p,LS}^H \mathbf{n}_p \quad (12)$$

Therefore the estimate vector $\hat{\mathbf{s}}_{p,LS}$ is a sample of an L -dimensional multi-variate complex Gaussian distribution with mean vector \mathbf{s}_p (the vector of transmitted signals) and covariance matrix $\mathbf{R}_{(\mathbf{s}_p - \hat{\mathbf{s}}_{p,LS})} \in \mathbb{C}^{L \times L}$ given by

$$\begin{aligned} \mathbf{R}_{(\mathbf{s}_p - \hat{\mathbf{s}}_{p,LS})} &= E\{(\mathbf{W}_{p,LS}^H \mathbf{n}_p)(\mathbf{W}_{p,LS}^H \mathbf{n}_p)^H\} \\ &= \sigma_n^2 (\mathbf{H}_p^H \mathbf{H}_p)^{-1} \end{aligned} \quad (13)$$

where σ_n^2 is the variance of the AWGN noise process at any receiving branch

$$E\{\mathbf{n}_p \mathbf{n}_p^H\} = \sigma_n^2 \mathbf{I} \quad (14)$$

According to (12) and (13), the l th user's associated mean-square error is given by the l th diagonal element of matrix $\mathbf{R}_{(\mathbf{s}_p - \hat{\mathbf{s}}_{p,LS})}$ [15]

$$\text{MSE}_{p,LS}^{(l)} = \sigma_n^2 \mathbf{w}_{p,LS}^{(l)H} \mathbf{w}_{p,LS}^{(l)} = \sigma_n^2 ((\mathbf{H}_p^H \mathbf{H}_p)^{-1})_{[l,l]} \quad (15)$$

The channel response estimation and the mean effective demodulator SNR of each received OFDM symbol can be used to determine the SNR at the p th subcarrier band as follows

$$\begin{aligned} \text{SNR}_p^{(l)} &= \frac{\sigma_l^2}{\text{MSE}_{p,LS}^{(l)}} = \frac{\overline{\text{MSE}}_{p,LS}^{(l)}}{\text{MSE}_{p,LS}^{(l)}} \overline{\text{SNR}}_{\text{eff}}^{(l)} \\ &= \frac{\overline{((\mathbf{H}_p^H \mathbf{H}_p)^{-1})_{[l,l]}}}{((\mathbf{H}_p^H \mathbf{H}_p)^{-1})_{[l,l]}} \overline{\text{SNR}}_{\text{eff}}^{(l)} \end{aligned} \quad (16)$$

where σ_l^2 is the l th user's associated transmit power or signal variance and this is constant over all subcarrier bands

$$E\{\mathbf{s}_p \mathbf{s}_p^H\} = \text{diag}(\sigma_1^2, \sigma_2^2, \dots, \sigma_L^2) \quad (17)$$

The sub-band SNR value can be compared with switching levels for picking out the modulation mode (including 'no transmission', i.e. $b_p = 0$) that ensures the instantaneous BER always remains below a certain threshold [13]. In addition, disabled subcarriers owing to low SNR values must carry on sending dummy data in order to compute their current sub-band SNR by means of (16). These dummy symbols can be known by receiver in order to

avoid an erroneous calculation of the effective demodulation SNR.

A further improvement can be carried out if subcarriers with higher SNR values between two switching levels are prompted to use the next modulation mode, whenever the average error probability does not overcome the imposed threshold [20]. Let be $b_p^{(l)}$ the number of bits conveyed by the p th subcarrier, and $P_p^{(l)}$ the bit error probability of the subcarrier when the modulation mode $2^{b_p^{(l)}}\text{-QAM}$ is used by the l th user, the average error probability is given by

$$P_{\text{avg}}^{(l)} = \frac{1}{B^{(l)}} \sum_{p=1}^{S_f} b_p^{(l)} P_p^{(l)}(b_p^{(l)}, \text{SNR}_p^{(l)}) \quad (18)$$

where $B^{(l)}$ is the total throughput of the l th user's adaptive system

$$B^{(l)} = \sum_{p=1}^{S_f} b_p^{(l)} \quad (19)$$

The bit error probability $P_p^{(l)}(b_p^{(l)}, \text{SNR}_p^{(l)})$ can be determined from the estimated signal-to-noise ratio of each sub-band ($\text{SNR}_p^{(l)}$) given by (16) and the BER curves against SNR obtained over AWGN channel [13, 15, 20]. Initially, the modulation modes of subcarriers are set up to those that overcome the switching levels for a certain target BER and then the modulation modes are successively increased for the 'best subcarriers' trying to augment $B^{(l)}$, while ensuring that $P_{\text{avg}}^{(l)}$ does not overcome the imposed BER threshold value. With the aim of maximising the total throughput $B^{(l)}$, while the average error probability $P_{\text{avg}}^{(l)}$ is maintained below the imposed maximum BER, we have adopted as criterion for selecting the 'best subcarriers' those that present a minimum increase in the next expression

$$\theta_{p,\Delta B}^{(l)} = \frac{(b_{p,\Delta B}^{(l)} P_{p,\Delta B}^{(l)} - b_p^{(l)} P_p^{(l)})}{(b_{p,\Delta B}^{(l)} - b_p^{(l)})} \quad (20)$$

where the values indicated with the subindex ΔB are referred to the new values of the parameters ($b_p^{(l)}$ and $P_p^{(l)}(b_p^{(l)}, \text{SNR}_p^{(l)})$) when the modulation mode of the p th subcarrier is increased to the next constituent modulation mode. When the 'best subcarrier' is selected by means of (20), the new average error probability given by (18) is re-calculated using the values referred to the new modulation mode and it is verified that the target BER is not overcome. If the previous condition is fulfilled, new 'best subcarriers' are looked for subsequently until the target BER is overcome. The selection criterion given by (20) is not optimum, but it allows to select with a high probability the 'best subcarriers' that maximising the total throughput with a minimum cost in the average error probability. Also, it is a very simple and efficient method that can be used in practical applications.

4 Simulation results

The IR channel configuration used in the study of the proposed system model is a furnished laboratory. The main characteristics of this laboratory are described in Table 1. The room has a wide variety of reflecting materials, including wood, glass (windows), cement and ceramic floor. The height of each piece of furniture is 1.60 m. The length of each one is 4.60 m and the width is 1.55 m. The pieces of furniture are distributed along the width of the room, and each one is separated by 1.75 m from each other. The

Table 1: Parameters for simulation

| Laboratory | Furniture | | |
|--|--------------------|-------|-----|
| Length (x): 5.80 m | Length (x): 4.60 m | | |
| Width (y): 13.25 m | Width (y): 1.55 m | | |
| Height (z): 3 m | Height (z): 1.60 m | | |
| Materials | ρ | r_d | m |
| Ceramic floor | 0.16 | 1 | – |
| Cement | 0.57 | 1 | – |
| Wood | 0.73 | 1 | – |
| Varnished wood | 0.75 | 0.3 | 97 |
| Glass | 0.03 | 0 | 280 |
| Resolution (Δt): 0.2 ns | | | |
| Simulation time (t_{max}): 100 ns | | | |
| Number of rays (N_R): 100 000 | | | |

locations of transmitters and receiver are specified in Fig. 3. The transmitters present three lobes of radiation modelled as ideal Lambertian of mode 2 (half-power beamwidth, HPBW = 45°), as portrayed in Fig. 3. The main lobe is pointed straight up and the other two lobes are tilted 45° with respect to the vertical. The receiver consists of six branches of equal FOV, $\phi_b = 40^\circ$. Each branch is made of a bare photodetector with a photosensitive area of 1 cm². For simplicity, the responsivity of the photodetectors is taken to be a constant, equal to 1 A/W. The central branch is oriented directly towards the ceiling and the five side branches are tilted 45° and distributed each 72° in azimuth uniformly, as depicted in Fig. 3. Table 2 summarises the main characteristics of emitters and receiver.

The previously described Monte Carlo ray-tracing algorithm [19] is used to calculate the channel impulse responses that there exist between the different transmitters and the detector's receiving branches. In general, the channel response at each branch consists of a set of sharp impulses of lower magnitude and higher spread when larger the length of the signal path between transmitter and receiver [21]. Thus, the greatest contribution in the signal power at receiver is due to user 3, while the most remote user 6 contributes with scarcely a tenth part in the signal power and it presents the most spread impulse responses at all six branches [21]. Moreover, if we consider user 1 as the desirable user, the most interfering users are user 3 and 2, respectively [21].

Several simulations were performed over previous multi-user optical communication system, assuming a transmission symbol rate of 1 Msymbol/s. The number of subcarriers is $N = 64$ (128-FFT), but only $S_f = 52$ convey data. A cyclic prefix extension of 32 samples was used, which leads to a transmission rate of 160 Msamples/s. An amplifier back-off value of 9 dB was considered since as a result of this it has been proved that the BER performance does not present differences with the non-limited case [13]. Furthermore, the training sequences used during the estimate of the channel impulse response are previously processed by the Rudin–Shapiro's method in order to improve the channel characterisation [13]. The transmitted OFDM signal bandwidth is <80 MHz and the cut-off frequency of used low-pass filters takes this value. The maximum achievable data rate for a particular user is 208 Mbits/s by using 16-QAM (4 bits by subcarrier symbol, 52 data subcarriers).

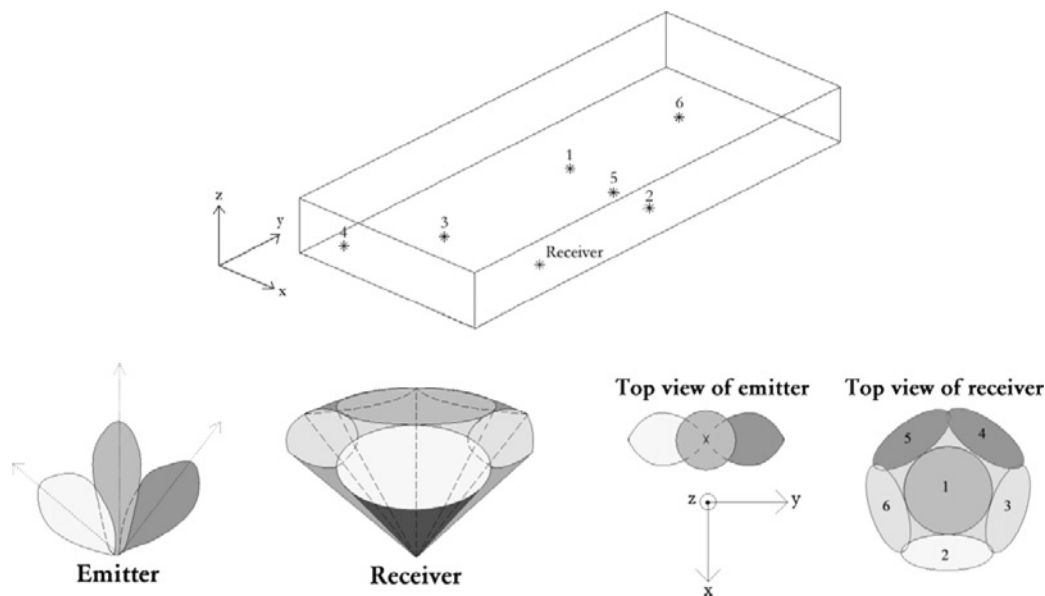


Fig. 3 Locations of the six transmitters and the receiver at the laboratory, and their structures

Fig. 4 shows the average throughput in bits per symbol (BPS) and BER obtained by the desirable user 1 against the average SNR value at the receiving branches using a four-mode ('no transmission', binary PSK, QPSK and 16-QAM) multi-user adaptive QAM scheme on a subcarrier-by-subcarrier basis, when different number of simultaneous users (L) share the optical medium. The results are represented as a function of the average channel SNR at receiving branches when we only consider the signal contribution relative to the desirable user 1 (the remainder users, that is, $l = 2, \dots, L$ also contribute in the total received signal power, increasing it when L augments, but we think it is more significant a performance representation against the signal power of the desirable user. A representation against the total signal power can lead to meaningless results because it produces a right shift of the curves that is greater when larger the number L of simultaneous users). The noise component is only referred to that induced by the optical channel or the photodetectors at receiver. The imposed threshold was 10^{-2} and ten training sequences were used to characterise the channel response. By using ten training sequences, the channel response estimation is very close to the actual channel response and the system performance is very similar to the ideal case, where a perfect knowledge of the channel response is considered [21]. Ten training sequences (TS = 10) have been used to estimate the channel response in all subsequent simulations. The results of Fig. 4 show that the multi-user adaptive system

maintains a near-constant BER close to the target BER (10^{-2}) until it reaches the highest-order modulation mode in all subcarriers (4 BPS). Then the BER drops dramatically because maximum achievable throughput is attained and the average SNR continues increasing. We can observe that when the number L of simultaneous users increases, the adaptive system requires a greater value of average SNR to achieve the 4 BPS throughput since it works in a noisier environment. In Fig. 5, we can observe the performance of the multi-user adaptive scheme when other target BER values are imposed. Newly, a near-constant BER and close to the imposed threshold are observed across a wide range of SNR values, while the maximum throughput is not reached. However, at very low SNR values the system cannot maintain the target BER since the noise level induced by the noise sources and the interfering users is too high and the system BER starts to increase rapidly.

The system performance can be compared with a fixed-mode system that uses the same modulation mode in every subcarrier [21]. The results have been obtained for both systems facing the same fixed configuration scenario previously described (Fig. 3). In Fig. 6, we cannot observe appreciable SNR gains (these hardly reach 2 dB excepting for $L = 6$ simultaneous users) with respect to the fixed-mode scheme due to the nearly constant effective frequency response of the studied indoor wireless optical channel, which is obtained thanks at the multi-branch angle-diversity receiver. However, the adaptive characteristics of the new scheme must be considered. The fixed-mode

Table 2: Parameters for emitters and receiver

| Emitters | | Receiver |
|----------------------------|-----------------------------------|-------------------------------------|
| Locations: (x y z), m | Radiation patterns | |
| Emitter 1: (2.9 6.6 1.6) | Mode (n): 2 | Position (x y z) m: (5.2 3.0 0.75) |
| Emitter 2: (5.2 7.0 0.75) | Number radiation lobes: 3 | Area: 1 cm ² |
| Emitter 3: (2.5 2.5 0.75) | Orientation (elevation, azimuth): | FOV: 40° |
| Emitter 4: (1.0 0.5 0.75) | (45° - 90°), (0° 0°), (45° 90°) | Orientation of detector branches |
| Emitter 5: (4.0 7.0 0.75) | | (elevation, azimuth): (0°, 0°), |
| Emitter 6: (2.5 11.0 0.75) | | (45°, 0°), (45°, 72°), (45°, 144°), |
| | | (45°, 216°), (45°, 288°) |

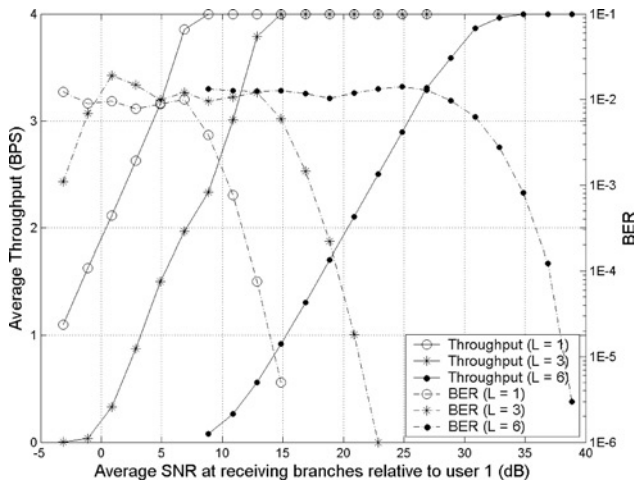


Fig. 4 Average throughput and BER of user 1's adaptive OFDM system when different number L of simultaneous users share the indoor wireless optical channel

scheme does not take into account the channel variations and number of simultaneous users, while the adaptive scheme attains to maintain a prefixed target BER although the environment features change. On the other hand, the adaptive system reaches the maximum achievable throughput at SNR values very close to those of the fixed-mode system. In Fig. 7, the performance of the new multi-user adaptive OFDM system in a single-user communication scenario ($L = 1$) is compared with that of the single-user adaptive OFDM system described in the work of González *et al.* [20]. Newly, the results have been obtained when both the single-user and the multi-user system face the same fixed configuration scenario, where now the remaining users ($l = 2, \dots, 6$) are 'inactive'. Average channel SNR gains > 8 dB are observed in this example, which is obviously attained by using a more complex receiver configuration in the new scheme (six demodulation branches). However, we must bear in mind that, except for the photodetectors and their associated electrical circuits, the OFDM demodulator can be shared by the P receiving branches by means of time-multiplexing and the remaining blocks of the receiver are common and very similar to that of the adaptive single-user detector [20]. Therefore the increase in the receiver complexity is not excessively significant and the transmitter structure has not been modified in the

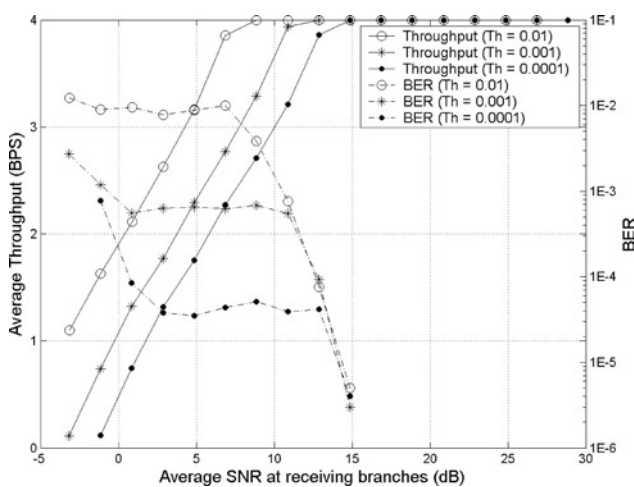


Fig. 5 Average throughput and BER of user 1's adaptive OFDM system for different values of target BER ($Th = 10^{-2}, 10^{-3}, 10^{-4}$) when single-user communications ($L = 1$) are considered

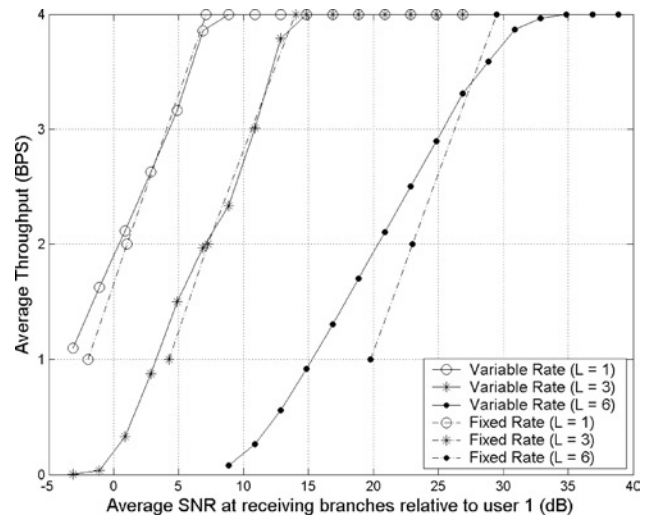


Fig. 6 Comparison of the average throughput of the adaptive scheme and the fixed-mode scheme

new proposed multi-user scheme either. Furthermore, the single-user OFDM system would not be able to face a multi-user scenario because it would incur in an irreducible BER.

Finally, Fig. 8 shows the performance of the actual multi-user adaptive system compared with that of an ideal system that presents a perfect knowledge of the channel response and the transmitted symbols. The good agreement between the results related to both systems indicates a near optimum performance of the new proposed scheme.

The previously shown results have been obtained assuming a fixed configuration of emitters and receiver, and user 1 as the desirable user. Other situations have been considered and we have found that the system throughput is very dependent on the emitters and receivers locations. However, the system is always able to provide the desired BER in spite of changes in the number of transmitting users and the positions of emitters and receivers around the room. Moreover, very significant SNR gains (> 7 dB) have always been observed with respect to the adaptive single-user scheme. As an example, in Fig. 9 we show the results obtained with the multi-user adaptive OFDM system when other users ($l = 2$ and $l = 3$) are considered

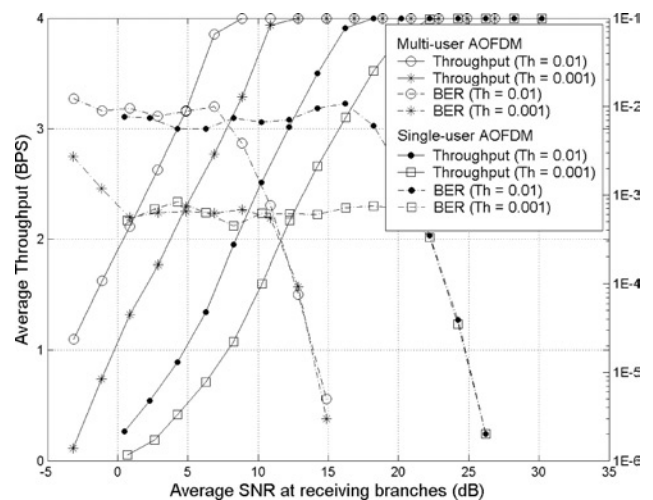


Fig. 7 BER performance improvement of the angle-diversity receiver assisted multi-user adaptive system when facing single-user communications, as compared with the previous system presented in the work of González *et al.* [20]

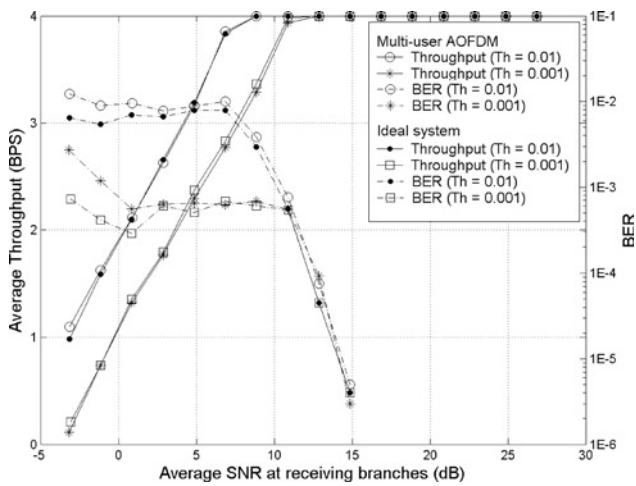


Fig. 8 Average throughput and BER of the multi-user adaptive scheme in a single-user scenario and the results when an ideal situation of perfect knowledge of the channel response and the transmitted symbols is considered

as the desirable user and the target BER is 10^{-2} . The results show that user 2 has a performance very close to that observed for the first user, and the third user presents a very good performance when it faces a scenario with $L = 3$ users. Its performance is very close to that obtained for $L = 1$. It is due to the significant difference between its channel responses at the receiving branches and the ‘spatial signatures’ of the remaining users [21], which makes its signal be little interfered by the other users. The multi-user adaptive scheme is also compared with the single-user adaptive scheme. SNR gains in excess of 7 dB can be observed. We have noticed similar performances of the remaining users ($l = 4, 5$ and 6) when a single-user scenario is faced. When a scenario with $L = 3$ simultaneous users is considered, the fifth and sixth users perform poorly because their signals are very weak (their transmissions are partially blocked up by furniture) with respect to the remaining interfering users. The fourth user performs almost as the third user because it has very distinct impulse responses with respect to the other users too.

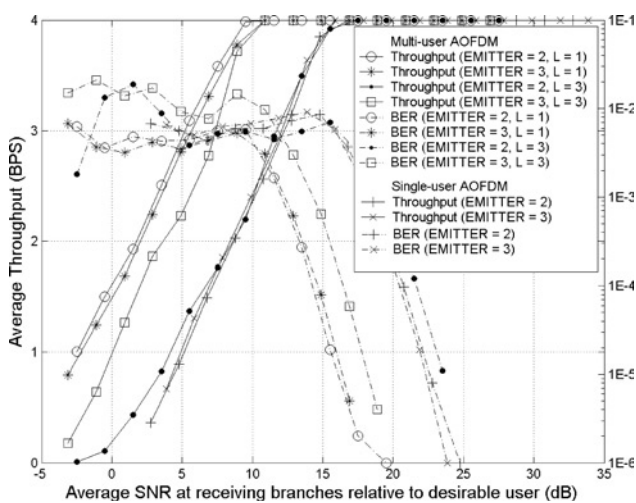


Fig. 9 Average throughput and BER of the multi-user adaptive scheme when considering $l = 2$ and $l = 3$ as the desirable user, and facing a scenario with $L = 1$ and $L = 3$ simultaneous users

The system performance is also compared with the previous single-user adaptive system presented in the work of González *et al.* [20], when it faces the same single-user environmental situation

5 Conclusions

In this paper, we have presented an adaptive SDMA–OFDM scheme for high bit rates multi-user communications over the indoor wireless optical channel. The proposed system employs the multi-user LS detection technique in a SDMA–OFDM scenario, in conjunction with angle-diversity reception. The designed multi-user system presents a significant performance improvement with respect to both a previous multi-user system and an adaptive single-user system, which is attained by means of a moderate increase in the system complexity. Signal-to-noise ratio gains in excess of 7 dB have been attained with respect to the previous single-user system, whereas the desirable BER rate remains nearly constant independently of either the channel fluctuations or the number of ‘active’ transmitter users. Moreover, the good system behaviour despite its simple structure let us consider that the use of more complex configurations of emitters and receivers, such as holographic optical systems, can offer significantly higher bit rates, even in more densely ‘populated’ scenarios.

6 Acknowledgment

This work has been funded in part by the Spanish Research Administration (TIC2003-07005).

7 References

- Kahn, J.M., Barry, J.R., Audeh, M.D., Carruthers, J.B., Krause, W.J., and Marsh, G.W.: ‘Non-directed infrared links for high-capacity wireless LANs’, *IEEE Pers. Commun. Mag.*, 1994, **1**, (2), pp. 12–25
- Kahn, J.M., and Barry, J.R.: ‘Wireless infrared communication’, *Proc. IEEE*, 1997, **85**, (2), pp. 265–298
- Barry, J.R., Kahn, J.M., Krause, W.J., Lee, E.A., and Messerschmitt, D.G.: ‘Simulation of multipath impulse response for wireless optical channels’, *IEEE J. Sel. Areas Commun.*, 1993, **11**, (3), pp. 367–379
- Kahn, J.M., Krause, W.J., and Carruthers, J.B.: ‘Experimental characterization of nondirected indoor infrared channels’, *IEEE Trans. Commun.*, 1995, **43**, (2/3/4), pp. 1613–1623
- Lomba, C.R., Valadas, R.T., and de Oliveira Duarte, A.M.: ‘Experimental characterisation and modelling of the reflection of infrared signals on indoor surfaces’, *IEE Proc., Optoelectron.*, 1998, **145**, (3), pp. 191–197
- López-Hernández, F.J., Pérez-Jiménez, R., and Santamaría, A.: ‘Ray-tracing algorithms for fast calculation of the channel impulse response on diffuse IR-wireless indoor channels’, *Opt. Eng.*, 2000, **39**, (10), pp. 2775–2780
- Audeh, M.D., Kahn, J.M., and Barry, J.R.: ‘Decision-feedback equalization of pulse-position modulation on measured nondirected indoor infrared channels’, *IEEE Trans. Commun.*, 1999, **47**, (4), pp. 500–503
- Wong, K.K., O’Farrell, T., and Kiatweerasakul, M.: ‘Infrared wireless communications using spread spectrum techniques’, *IEE Proc., Optoelectron.*, 2000, **147**, (4), pp. 308–314
- Carruthers, J.B., and Kahn, J.M.: ‘Angle diversity for nondirected wireless infrared communication’, *IEEE Trans. Commun.*, 2000, **48**, (6), pp. 960–969
- Akhavan, K., Kavehrad, M., and Jivkova, S.: ‘High-speed power-efficient indoor wireless infrared communication using code combining – Part I’, *IEEE Trans. Commun.*, 2002, **50**, (7), pp. 1098–1109
- Kavehrad, M., and Jivkova, S.: ‘Indoor broadband optical wireless communications: optical subsystems designs and their impact on channel characteristics’, *IEEE Wirel. Commun.*, 2003, **10**, (2), pp. 30–35
- Carruthers, J.B., and Kahn, J.M.: ‘Multiple-subcarrier modulation for nondirected wireless infrared communication’, *IEEE J. Sel. Areas Commun.*, 1996, **14**, (3), pp. 538–546
- González, O., Pérez-Jiménez, R., Rodríguez, S., Rabadán, J., and Ayala, A.: ‘OFDM over indoor wireless optical channel’, *IEE Proc. Optoelectron.*, 2005, **152**, (4), pp. 199–204
- Hara, S., and Prasad, R.: ‘Overview of multicarrier CDMA’, *IEEE Commun. Mag.*, 1997, **35**, (12), pp. 126–133

- 15 Hanzo, L., Münster, M., Choi, B.J., and Keller, T.: 'OFDM and MC-CDMA for broadband multi-user communications, WLANs and broadcasting' (John Wiley & Sons, West Sussex, England, 2003)
- 16 Vandenameele, P., Van Der Perre, L., Engels, M.G.E., Gyselinckx, B., and De Man, H.J.: 'A combined OFDM/SDMA approach', *IEEE J. Sel. Areas Commun.*, 2000, **18**, (11), pp. 2312–2321
- 17 Thoen, S., Deneire, L., Van der Perre, L., Engels, M., and De Man, H.: 'Constrained least squares detector for OFDM/SDMA-based wireless networks', *IEEE Trans. Wireless Commun.*, 2003, **2**, (1), pp. 129–140
- 18 Rodríguez, S., Pérez-Jiménez, R., López-Hernández, F.J., González, O., and Ayala, A.: 'Reflection model for calculation of the impulse response on IR-wireless indoor channels using ray-tracing algorithm', *Microw. Opt. Technol. Lett.*, 2002, **32**, (4), pp. 296–300
- 19 González, O., Rodríguez, S., Pérez-Jiménez, R., Mendoza, B.R., and Ayala, A.: 'Error analysis of the simulated impulse response on indoor wireless optical channels using a Monte Carlo based ray tracing algorithm', *IEEE Trans. Commun.*, 2005, **53**, (1), pp. 124–130
- 20 González, O., Pérez-Jiménez, R., Rodríguez, S., Rabadán, J., and Ayala, A.: 'Adaptive OFDM system for communications over the indoor wireless optical channel', *IEE Proc., Optoelectron.*, 2006, **153**, (4), pp. 139–144
- 21 González, O.: 'Estudio de la aplicación de técnicas de modulación OFDM para comunicaciones ópticas no guiadas en el canal infrarrojo', PhD thesis, University of La Laguna, 2005